



# Semiautomated Software to Improve Stability and Reduce Operator-Induced Variation in Vascular Ultrasound Speckle Tracking

Nirmala Rajaram, PhD , Brian J. Thelen, PhD, James D. Hamilton, PhD, Yihao Zheng, PhD, Timothy Morgan, PhD, Miguel Angel Funes-Lora, PhD, Lenar Yessayan, MD, Albert J. Shih, PhD, Peter Henke, MD, Nicholas Osborne, MD, Brandie Bishop, RV, Venkataramu N. Krishnamurthy, MD, William F. Weitzel, MD 

Received October 18, 2021, from the Veterans Affairs Ann Arbor Healthcare System, Ann Arbor, Michigan, USA (N.R., B.J.T., J.D.H., Y.Z., L.Y., P.H., N.O., B.B., V.N.K., W.F.W.); Department of Psychiatry, University of Michigan, Ann Arbor, Michigan, USA (N.R.); Department of Statistics, University of Michigan, Ann Arbor, Michigan, USA (B.J.T.); Michigan Tech Research Institute, Michigan Technological University, Ann Arbor, Michigan, USA (B.J.T.); Department of Mechanical Engineering, Worcester Polytechnic Institute, Worcester, Massachusetts, USA (Y.Z.); John D. Dingell Veterans Affairs Medical Center, Detroit, Michigan, USA (T.M.); Department of Mechanical Engineering, University of Michigan, Ann Arbor, Michigan, USA (M.A.F.-L., A.J.S.); Department of Internal Medicine, University of Michigan, Ann Arbor, Michigan, USA (L.Y., W.F.W.); Department of Surgery, University of Michigan, Ann Arbor, Michigan, USA (P.H., N.O.); and Department of Radiology, Case Western Reserve, Cleveland, Ohio, USA (V.N.K.). Manuscript accepted for publication January 18, 2022.

We acknowledge Dr. Scott Buchowski, Jingxuan L, Patricia Rose, Jesse Winters, and Ariel Zalesin who helped us evaluate the open-source software.

This work was supported in part by the United States Office of Veterans Affairs (grant number SI01RX002271).

All of the authors of this article have reported no disclosures.

Address correspondence to Nirmala Rajaram, PhD, VA Ann Arbor Health System (151), 2215 Fuller Road, Ann Arbor, MI 48105, USA.

E-mail: [nirmala@umich.edu](mailto:nirmala@umich.edu)

doi:10.1002/jum.15960

**Objectives**—Ultrasound is useful in predicting arteriovenous fistula (AVF) maturation, which is essential for hemodialysis in end-stage renal disease patients. We developed ultrasound software that measures circumferential vessel wall strain (distensibility) using conventional ultrasound Digital Imaging and Communications in Medicine (DICOM) data. We evaluated user-induced variability in measurement of arterial wall distensibility and upon finding considerable variation we developed and tested 2 methods for semiautomated measurement.

**Methods**—Ultrasound scanning of arteries of 10 subjects scheduled for AVF surgery were performed. The top and bottom of the vessel wall were tracked using the Kanade-Lucas-Tomasi (KLT) feature-tracking algorithm over the stack of images in the DICOM cine loops. The wall distensibility was calculated from the change of vessel diameter over time. Two semiautomated methods were used for comparison.

**Results**—The location of points selected by users for the cine loops varied significantly, with a maximum spread of up to 120 pixels (7.8 mm) for the top and up to 140 pixels (9.1 mm) for the bottom of the vessel wall. This variation in users' point selection contributed to the variation in distensibility measurements (ranging from 5.63 to 41.04%). Both semiautomated methods substantially reduced variation and were highly correlated with the median distensibility values obtained by the 10 users.

**Conclusions**—Minimizing user-induced variation by standardizing point selection will increase reproducibility and reliability of distensibility measurements. Our recent semiautomated software may help expand use in clinical studies to better understand the role of vascular wall compliance in predicting the maturation of fistulas.

**Key Words**—arteriovenous fistula; kidney disease; semiautomated; speckle tracking; ultrasound; vascular distensibility

Arteriovenous fistula (AVF) is the preferred vascular access for hemodialysis treatment in patients with chronic kidney disease (CKD) and end-stage renal disease (ESRD).<sup>1,2</sup> Unfortunately, about 20 to 60% of AVFs fail to mature sufficiently to sustain dialysis.<sup>3,4</sup> Repeated surgical interventions or creation of a new fistula increases morbidity and medical costs and may adversely affect quality of life for patients.<sup>5,6</sup>

Ultrasound imaging has been used to identify factors that may affect clinical AVF maturation. The efficacy of preoperative and early postoperative studies involving duplex ultrasound scanning of vessels<sup>7</sup> and the role of volume flow rate, vein distensibility, arterial and vein size<sup>8–11</sup> in predicting AVF maturation are being investigated. A postoperative evaluation up to 6 weeks after fistula creation reported that AVF blood flow, diameter, and depth may moderately predict unassisted and overall AVF clinical maturation.<sup>12,13</sup> Diagnostic tools that can successfully predict functional AVF maturation are critical to improve the prognosis and treatment of CKD and ESRD patients.<sup>7,10,13</sup>

We have developed novel ultrasound software that allows investigation of vascular mechanics clinically.<sup>14–18</sup> This software uses standard ultrasound Digital Imaging and Communications in Medicine (DICOM) data to measure circumferential vascular wall strain (distensibility) based on speckle tracking techniques. The software allows measurements of distensibility within single and multiple cardiac cycles and can be used to track changes in wall compliance as the AVF matures.<sup>14,15</sup>

Ultrasound elastography has been widely used in the medical field to evaluate liver fibrosis and to differentiate between benign and malignant lesions in breast, thyroid, and prostate.<sup>19–22</sup> There is also significant potential for ultrasound elastography to be useful in the vascular access and peripheral vascular setting.<sup>14,15,23–29</sup> However, intraoperator and interoperator variability in ultrasound measurements has always been a concern as indicated by studies in various organs.<sup>30–38</sup> For example, operator-dependent measurement and interpretation greatly influence the assessment of fetal growth, an essential component of prenatal care, facilitating the identification of fetuses at risk of perinatal morbidities or mortality.<sup>32,39</sup> In the noninvasive assessment of endothelial function in cardiovascular disease using flow-mediated dilation (FMD) technique, operator-based variability in ultrasound measurements of peripheral artery endothelium-dependent dilation significantly impairs its reproducibility and comparison between studies.<sup>26</sup> Therefore, it is imperative to identify user-based errors and establish a standard data acquisition system and guidelines to enable accuracy and reproducibility of ultrasound imaging to have a positive clinical impact. To this end, we conducted an analysis of operator-induced variation in the clinical setting and

studied 2 potential solutions aimed at standardizing user input and measurement methods.

The 2 main operator-sourced factors that can affect the accuracy of our speckle tracking-based software to measure vascular mechanical properties are: (1) proper and stable placement of the transducer on the subject's fistula for recording and (2) the software user interface calipers selected within the ultrasound image by the user to obtain accurate measurements of the wall strain. In this study, we address the second potential source of variation. To do so, we evaluated the variability of the wall strain (distensibility) measurements as a function of user-induced variation in point selection of the top and bottom edge of arterial vessel walls (using our previously developed method),<sup>14–17</sup> as well as the physiologic variation in wall strain attributable to beat-to-beat (BTB) variation in pulse pressure. Observing a significant degree in measurement variation arising from the users' variation in point selection, we devised software-assisted measurement systems that implement semiautomated methods for vessel edge detection and strain peak and valley measurement. The purpose was to define and test algorithms and software for measurement standardization to increase the reproducibility and reliability of automated measurement of vessel wall distensibility in preparation for larger-scale clinical testing.

## Materials and Methods

### Subjects

We enrolled 10 subjects (67–88 years) with ESRD who were scheduled to undergo surgery to create an AVF. This study was approved by the local Veterans Affairs Ann Arbor Healthcare System's Institutional Research Board and a written informed consent was obtained from all participants.

### Wall Strain (Distensibility)

Strain describes the deformation of an object. For instance, the normal Lagrangian strain can be defined as the ratio of the change in length to its original length. The circumferential vessel wall strain, given the cylindrically symmetric vessel wall geometry, is the change in circumference of a vessel wall divided by the original circumference. Since the circumference is linearly related to the diameter of the vessel,

this is equal to the ratio of the change in diameter divided by the original diameter.

As illustrated in Figure 1, following cardiac cycles, the blood pressure (BP) varies periodically with the peak and valley being the systolic pressure ( $P_s$ ) and diastolic pressure ( $P_d$ ), respectively. Given the linear relationship between BP and the vessel circumferential stress,<sup>40</sup> the vessel circumference changes with the BP and the vessel diameter varies between the systolic diameter ( $D_s$ ) and diastolic diameter ( $D_d$ ), accordingly. The vessel circumferential strain can be expressed as:

$$\varepsilon = \frac{(\pi D_s - \pi D_d)}{\pi D_d} = \frac{(D_s - D_d)}{D_d} \quad (1)$$

and we define Equation (1) as the distensibility of the vessel wall.

#### Ultrasound Data Acquisition

A GE LOGIQ E9 ultrasound system (LOGIQ E9 XD Clear 2.0, General Electric Healthcare, Waukesha, WI) was used to scan the subject's inflow artery (brachial/radial); cine loop data were collected for a standard data capture time of 10 seconds at a frame rate of 33 Hz for 9 subjects (with a 9 L-D broad-spectrum

linear transducer; band width of 2–8 MHz) and 17 Hz for one subject (with a L-8-18i-D broad-spectrum linear hockey stick transducer; band width of 4–15 MHz) from B-mode images in short-axis views of the artery; and DICOM data were exported for processing.

#### Postprocessing and Analysis

Our previously developed open source software<sup>14,15</sup> was used to measure circumferential vascular wall strain or distensibility (tracking vessel wall diameter changes over time) of brachial and radial arteries using standard ultrasound DICOM cine loop data.

To enable an optimal evaluation and reduce bias in the selection of points, these studies were performed by users that were not involved in the software design. The users were research personnel and included 4 clinicians. The users applied our open-source software based on ultrasound speckle tracking to obtain distensibility measurements for ultrasound cine loops of arteries from 10 different subjects (Table 1). Each user had individualized training with the first author of the manuscript to learn how to use the software. Once several sample cases were observed, and the users did not require any more trainer input, they were allowed to perform the study

**Figure 1.** Circumferential vascular wall strain (distensibility,  $\varepsilon$ ): Defined as the ratio of the change in vessel diameter, the difference between diastolic diameter ( $D_d$ ) and systolic diameter ( $D_s$ ), during a cardiac cycle, to the original diastolic diameter.

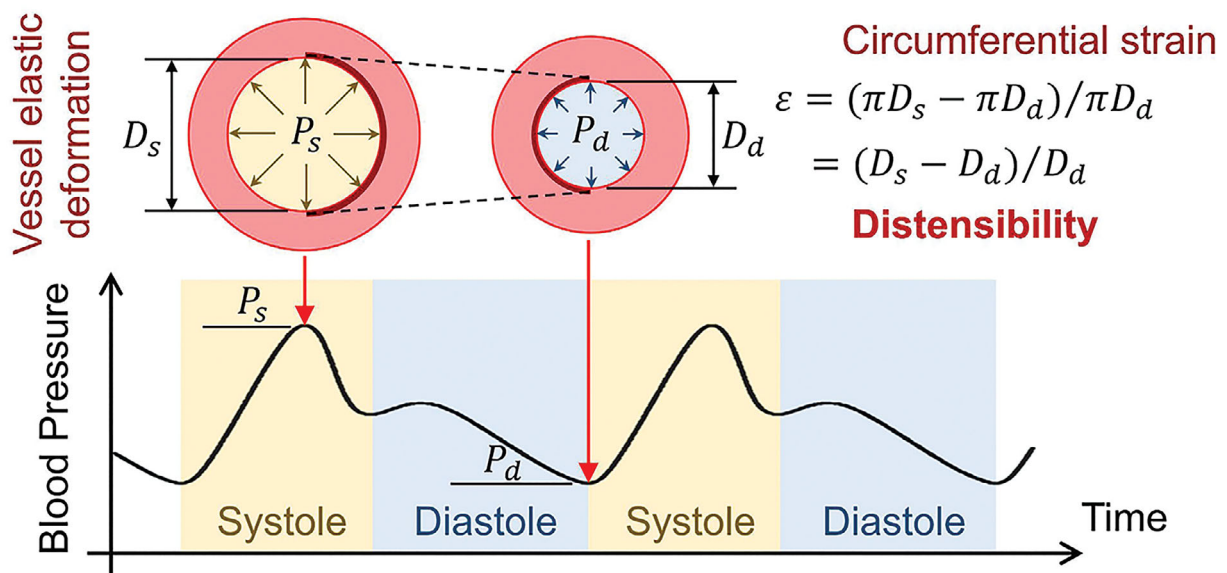


**Table 1.** Distensibility and Relative Beat-to-Beat Variation

Effect of Variation in Point Selection by Users		1	2	3	4	5	6	7	8	9	10	
Subject #		14	10	15	12	120	20	20	10	12	7	
Maximum spread in top position (pixels)		20	7	14	7	140	16	30	5	8	10	
Maximum spread in bottom position (pixels)		2.07	2.16	2.83	2.32	2.43	2.49	4.87	5.77	2.5	6.09	
Median distensibility (%)		2.39 ± 0.98	2.152 ± 0.21	2.84 ± 0.16	2.312 ± 0.19	2.46 ± 0.27	2.53 ± 0.37	5.04 ± 0.55	5.929 ± 0.69	2.583 ± 0.31	6.061 ± 0.38	
Mean distensibility (%) ± SD		41.04	9.76	5.63	8.22	15.07	10.66	10.91	11.64	12.00	6.27	
User-induced distensibility variation (%)		15.81	11.9	17.55	12.26	17.68	7.16	15.89	10.23	6.41	14.38	
Relative beat-to-beat variation (BBV %)		<b>Use of CED-PD-MT semiautomated method</b>										
Distensibility (%)		2.55	2.75	3.74	2.60	3.44	2.89	5.81	6.59	3.59	7.50	
Relative beat-to-beat variation (BBV %)		13.88	13.90	17.58	26.28	13.11	7.52	12.19	15.04	4.55	14.96	
Distensibility (%)		<b>Use of SED-LD-FT semiautomated method</b>										
Distensibility (%)		3.10	2.49	3.65	3.02	2.64	2.85	7.97	6.77	4.47	8.60	
Relative beat-to-beat variation (BBV %)		18.38	16.15	12.37	16.85	19.58	7.07	23.64	14.77	6.34	23.77	

BBV indicates beat-to-beat variation; CED-PD-MT, Canny edge detector-polynomial detrending-manual thresholding; SED-LD-FT: Sobel edge detector-polynomial detrending-fixed thresholding.

measurements on the test cases. The user interface of the software requires the user to select a position at the top and bottom of the vessel wall (the lumen-vessel wall interface) to measure distensibility as a function of time. To maintain consistency in the measurement of vessel distensibility, the 10 users were instructed to choose 2 points along an imaginary vertical line in the center of the vessel in the first frame of the ultrasound cine loop. The 2 selected points were tracked using the KLT feature tracking algorithm over the acquisition period. The point selection was repeated in case of loss of tracking.

The vessel diameter (distance between 2 points) was computed over the entire stack of images and a graph of the change in vessel wall diameter (cm) over time (secs) was plotted. To generate a more representative distensibility measurement, we asked each user to select 6 consecutive peaks (systolic/maximum diameters) and valleys (diastolic/minimum diameters) from the waveform and the mean of the vessel diameters was used to determine the wall strain or distensibility of the vessel wall. After linear signal detrending (based on 6 selected peaks and valleys), the vessel distensibility ( $\epsilon$ ) was computed as in Equation (1).

The statistical analysis for this study mainly focused on subject-specific statistics computed across 10 users. The median and mean distensibility were computed for each subject across all 10 users, along with the standard deviation. We also reported relative distensibility variation (user-induced distensibility variation, %), via normalizing the standard deviation by mean distensibility.

The beat-to-beat variation (BBV) across all 6 peaks and valleys was defined as standard deviation of all the peaks (systolic diameter,  $D_s$ ) minus the adjacent valleys (diastolic diameter,  $D_d$ ) measurements (relative to that peak) normalized to the mean of diastolic diameters ( $D_d$ ):

$$BBV = \frac{1}{D_d} \times Std\ Dev\{ \{(D_{si} - D_{di})\}_{i=1}^6, \{(D_{si+1} - D_{di})\}_{i=1}^5 \} \times 100\% \quad (2)$$

The relative BBV is derived by normalizing the BBV to distensibility ( $\epsilon$ ):

$$Relative\ BBV = \frac{BBV}{\epsilon} \quad (3)$$

### Semiautomated Methodology

To reduce user input variation, we developed algorithms to standardize the areas requiring user input including vessel edge point selection and distensibility waveform peak and valley selection. We implemented and evaluated 2 methods of semiautomation for comparison with the baseline user input data. The automated methodology is flexible in its implementation, and we summarize the 2 different approaches tested in this study.

#### Method 1: Canny Edge Detection-Polynomial Detrending-Manual Thresholding Method

For method 1, we implemented the Canny edge detection-polynomial detrending-manual thresholding (CED-PD-MT) method that was developed in a previous study.<sup>18</sup> This method starts with the user defined manual point selection and subsequently processes the vessel using filtering, segmentation, and automated edge detection prior to speckle tracking.<sup>18</sup> To briefly summarize, coding for this method was implemented using MATLAB (MathWorks, Natick, MA), and the threshold was

adjusted manually to sharpen the lumen boundary in the CED-PD-MT method by the software operator. Then, the initial frame was extracted from the cine-loop DICOM data and binarized.<sup>41,42</sup> Next, the user selected the center of the vessel of interest. A Canny edge detector identified the vessel contour by implementing smoothing, non-maximal suppression, and hysteresis.<sup>43–45</sup> To adjust for factors that lead to fluctuations in peaks and valleys such as transducer motion, fluctuations in stroke volume and BTB BP changes, we implemented a low order polynomial fit and subtracted this signal from the original displacement<sup>18</sup> to detrend the signal. The consecutive peaks and valleys resulting from vessel distention were then approximated using penalized least squares and the direct and inverse discrete cosine transform to obtain a smoothed displacement signal defined as a low order polynomial.<sup>18</sup>

#### Method 2: Sobel Edge Detection-Linear Detrending-Fixed Thresholding Method

For method 2, we implemented many of the steps as in method 1, with the primary differences being

**Figure 2.** Cross-sectional view of arteries in the left panels with a magnified view (3.5X) of arteries in the right panels: The location of points chosen by 10 users (represented by different colors) at the top and bottom of the arterial wall on the first frame of the ultrasound cine loop of subject #8 (top panel; minimum variation) and of subject #5 (bottom panel; maximum variation).

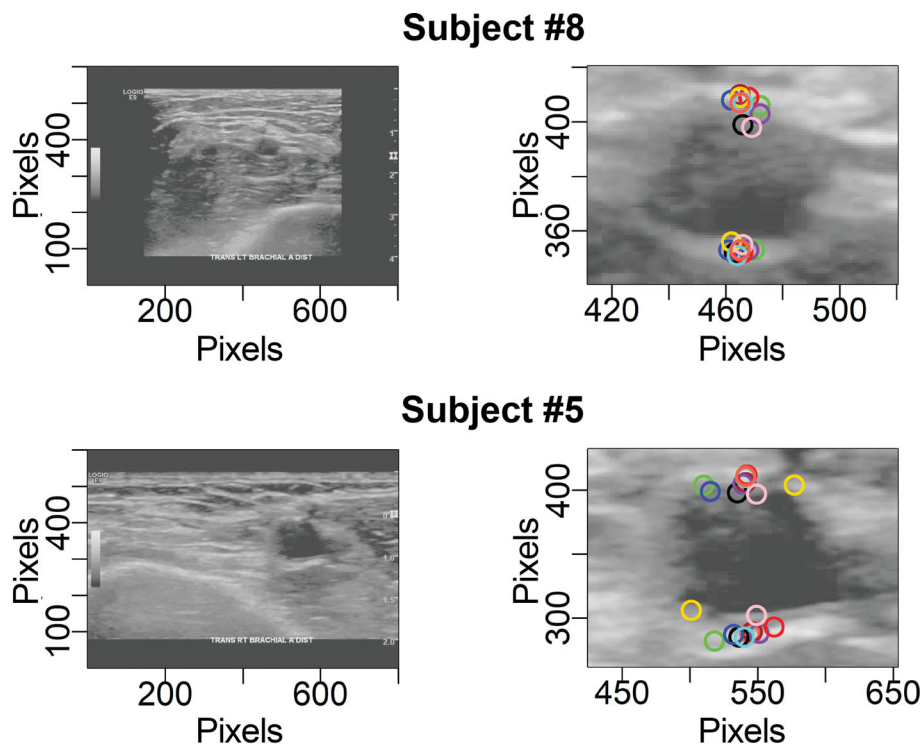
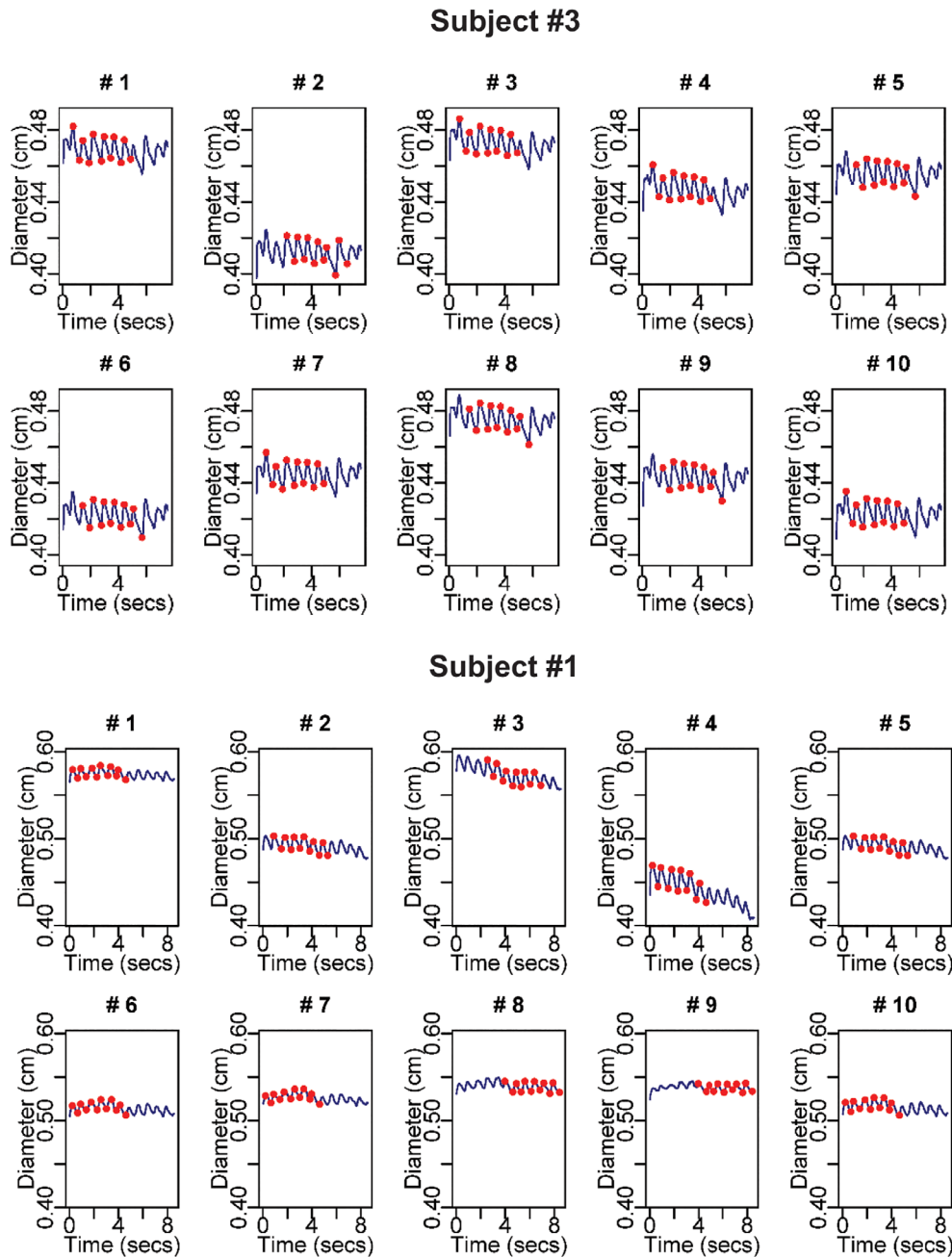


**Figure 3.** Minimum (subject #3) and maximum (subject #1) variation in distensibility: Wave plots (change in diameter of vessel wall over time) based on locations of points chosen by 10 users (#1–#10). Six sequential peaks and valleys marked by the users are shown in red.



(1) using a Sobel edge detector instead of a Canny edge detector,<sup>46</sup> (2) linear detrending instead of polynomial detrending, and (3) preset thresholding (no manual adjustment by the user). The coding

environment was open-source Python Libraries (Python Software Foundation, Beaverton, OR). Additionally, the peak and valley determinations were performed by providing a preset parameter for the minimum

peak and valley separation distance, which is dependent on the frame rate used to acquire the ultrasound data, and by providing a median filter window size for the distensibility signal waveform that resulted from speckle tracking. A modification of the KLT algorithm by Farneback<sup>47</sup> was implemented for speckle tracking for the Sobel Edge Detection-Linear Detrending-Fixed Thresholding (SED-LD-FT) data analysis. Standard Python libraries<sup>48</sup> were used for segmentation, signal processing, peak, and valley selection.

## Results

### *Interuser Variation Exists in Point Selection*

There was significant variation in the location of points selected by the users for the ten cine loops, with a maximum spread of up to 120 pixels (7.8 mm) for the top and up to 140 pixels (9.1 mm) for the bottom of the vessel wall as shown in Table 1 (first 2 rows). The cross-sectional view of the arteries in Figure 2 shows the spread of the locations of top and bottom points in the first frame of the ultrasound cine loop. There was minimum variation in user selection of the 2 points for subject #8 (top panel in Figure 2; Table 1) and a maximum variation for subject #5 (bottom panel in Figure 2; Table 1).

### *Interuser Variation in Point Selection Affects Distensibility Measurements*

Table-1 shows the distensibility measurements done by the 10 users for the ultrasound cine loops of arteries from 10 subjects. The median distensibility of the 10 arterial walls ranged from 2.07 to 6.09% (Table 1). The variation in distensibility ranged from 5.63 to 41.04% for the 10 arteries across users (Table 1). Figure 3 shows a graph of the change in vessel wall diameter (cm) over time (seconds). These wave plots of change in diameter versus time showed a maximum variation in distensibility of 41.04% for subject #1, and a minimum variation in distensibility measurement of 5.63% for subject #3 (Table 1; Figure 3). The high variation in distensibility measurements of the arterial wall of subject #1 seemed to largely be due to a single outlier value (based on the selection of points on the lumen-vessel wall interface) by user #4 as shown in Figure 3. Even if we exclude that value, subject #1 continues to show the most variation in distensibility.

The variation in point selection by users did not directly translate to the same extent in variation of the

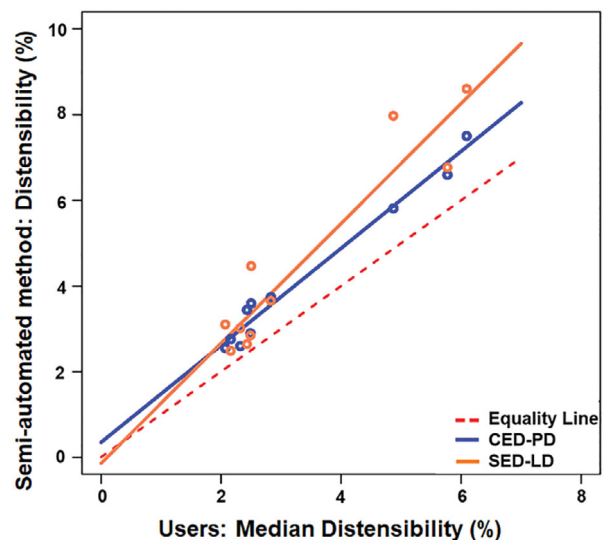
distensibility measurements of the arterial walls. However, subject #5 who had the maximum variation in location selection (Table 1; Figure 2) by the 10 users also showed a high variation in distensibility (15.07%; Table 1). Subject #8 which showed minimum variation in location selection (Table 1; Figure 2) showed a slightly lower variation in distensibility (11.64%; Table 1).

### *Interuser Variation in Point Selection Contributes to Variation in Beat-To-Beat Measurements*

The BBV in BP is well described and attributable in part to respiratory modulation of intrathoracic pressure, and accentuated with irregular heart rhythms.<sup>49,50</sup> As the driving force (BP) for distensibility varies, the effects (wall strain or distensibility) may be measured using this method. So, the effects of BBV in BP may be observed as BBV in distensibility.

The BTB measurements were obtained from different cycles (peaks and valleys; Figure 3) for all subjects across the different users (Table 1). The relative BBV ranged from 6.41 (subject# 9) to 17.68% (subject# 5). Subject# 5 who showed a maximum variation in point selection by users (Figure 2; Table 1) also exhibited a maximum BBV (17.68%; Table 1) and a high variation

**Figure 4.** Regression analysis comparing the distensibility obtained by the 2 semiautomated methods Canny edge detector-polynomial detrending-manual thresholding (CED-PD-MT, blue) and Sobel edge detector-polynomial detrending-fixed thresholding (SED-LD-FT; red) with the median distensibility obtained by the 10 users.



in distensibility (15.07%; Table 1). The inter-user variation in point selection contributed to variation in both BTB and distensibility (wall strain) measurements.

**Semiautomated Methods Have Potential to Reduce User-Induced Variation**

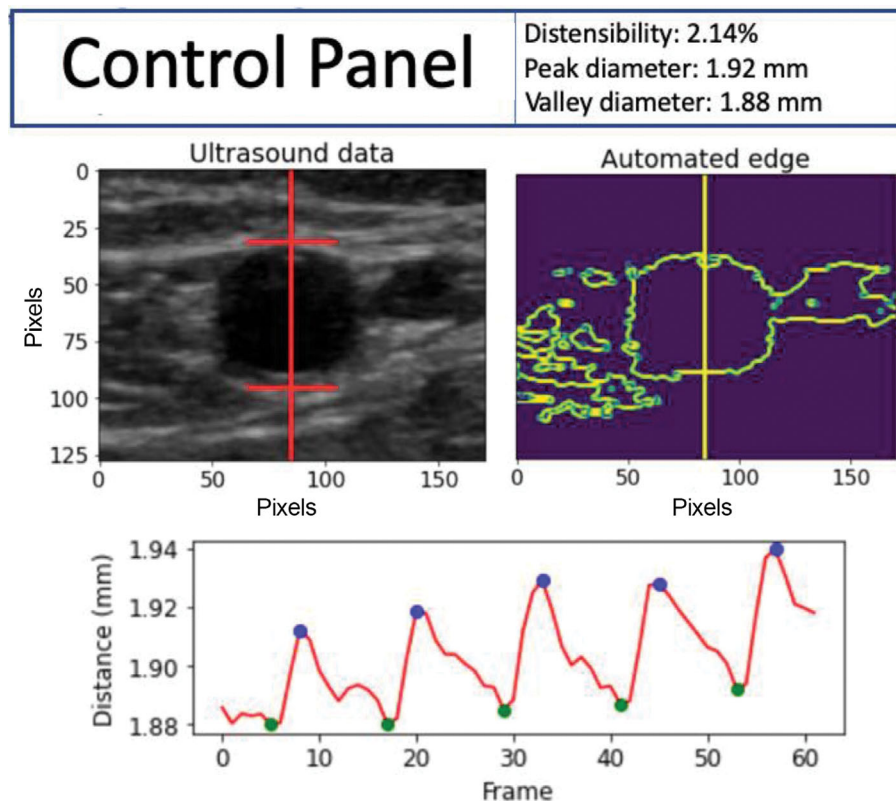
Both semi-automated approaches (CED-PD-MT and SED-LD-FT) showed a strong correlation with the median user input-based results, with a correlation co-efficient of 0.9758 for CED-PD-MT method and 0.8928 for SED-LD-FT method (Figure 4). Additionally, both methods were on average higher than the user input-based results (Table 1; Figure 4). It is important to note that the BBV in measurements was preserved in both semi-automated methods (Table 1), while showing the potential to reduce user-induced variation. Preserving the ability to detect this physiologic variation while reducing operator-induced variation will allow additional future testing of pressure induced strain variation using semiautomated

methods. In addition to testing semiautomated methods that may help further testing, we developed a user-friendly browser-based user interface. Figure 5 shows the interface implementing the SED-LD-FT method.

**Discussion**

The development of a vascular diagnostic system which can accurately measure parameters that can guide the creation of a successful AVF and its maturation will be beneficial to patients with CKD and ESRD undergoing maintenance hemodialysis.<sup>7,10,13</sup> Our previous open-source ultrasound software based on speckle tracking algorithms has shown significant potential in detecting changes in vascular mechanics in the postoperative period following dialysis fistula creation.<sup>14-18</sup> To evaluate and enhance the reliability and accuracy of the application of the software in a

**Figure 5.** User interface (UI) under development allows users to identify the ultrasound data to be analyzed (upper left) with automated edge detection (upper right) and motion tracking to determine maxima (peaks) and minima (valleys) (lower graph) and results (upper right corner).





clinical setting, we conducted this study to understand the effect of user-induced and physiologic (BTB) variation on vascular distensibility. Upon finding significant user input-induced variation, we sought to develop and evaluate methods that may standardize the measurement and allow more widespread testing.

An important initial finding which corroborates our earlier studies is that the software efficiently determined the circumferential vessel wall strain (distensibility) using the speckle tracking algorithm on standard DICOM images.<sup>14,15,17</sup> The measurement of small changes in the motion of vessel walls with high resolution is encouraging since we used conventional ultrasound scanners and open-source DICOM data available to any clinician.

For a successful application of the existing open-source software, it is important to carefully choose 2 points of interest at the top and bottom of the vessel wall which will be tracked to compute vessel diameter during speckle tracking. In the user input portion of the study, even though we set a basic rule for point selection, where the 10 users were instructed to choose 2 points at the vessel edge and along the central axis of the vessel in the first frame of the ultrasound cine loop, there was variation in point selection across users which resulted in distensibility measurement variation. In an extreme case, the cine loop data collection for subject #5 had considerable motion intermittently throughout the data due to transducer instability at the time of ultrasound data collection. It is likely that this contributed to the very large variation in point selection by the users, who may have had to move away from the axis along the center of the vessel to choose the points to avoid loss of speckle tracking. The second possible source of variation by the user is in the selection of 6 sequential peaks and valleys in the distensibility waveform plot (diameter versus time) to compute distensibility values. To address these variations, we developed and tested 2 semiautomated methods, addressing both user point selection and peak/valley selection. Both automated methods replace individual user input with established but different thresholding and edge detection algorithms and automated algorithms for peak and valley selection. Interestingly, both semiautomated methods were highly correlated with the median user input results. Another interesting observation was that

the results of both semiautomated methods averaged higher than the user input-derived results. We speculate that, in the user input study, the user may tend to select points that move less to improve the waveform and tracking, leading to lower distensibility measurements, a possible source of biasing in the user input method toward lower values. It is also possible that the semi-automated methods tended to select points closer to the vessel lumen which is the subject of an ongoing study. These points may move more than points further away from the vessel edge, increasing the semiautomated distensibility measurements. In addition, these points will have a smaller baseline diameter that will tend to increase the distensibility measurement. In either case, the diagnostic thresholds for distensibility have not been established, and having a reliably repeatable measurement is crucial for clinical study, even at the expense of a measurement bias. Nevertheless, these potential sources of measurement bias require additional investigation and we have plans for laboratory studies to evaluate them further.

Based on our analysis, variation in distensibility measurement is not only influenced by variation in user point selection but also by physiologic BBV. Interestingly, both BBV and variation in point selection by users contribute to the variation in distensibility with a similar degree. This raises the possibility of implementing protocols or algorithms that can standardize point selection, minimizing user introduced variation while allowing for physiologic BBV in distensibility, which could have diagnostic utility. Distensibility may be a dynamic variable, related to the underlying BP, heart rate, and pulse pressure, as well as the mechanical properties of the vessel wall. Both semiautomated methods preserved the BBV in measurements while showing the potential to reduce user-induced variation. Further study is in progress to understand which components of these automation strategies, edge detection, detrending, and/or thresholding most influence the performance differences.

Also, the arterial waveform plots (change of diameter of vessel wall over time) in our study indicates that variation observed in raw distances is less than variation in distensibility measurements. This too is an important observation and results from the diameter (baseline distance) varying more than the vessel wall excursion. Even though the transducer was placed gently, the surface transducer pressure may subtly compress the vessel, changing baseline diameter and influencing the

denominator of the distensibility measurement. While transducer effects were not evaluated in this study, this is another variable that must be standardized. Given the nonlinear vascular wall elasticity,<sup>24,27</sup> the same pulse pressure may result in a greater distance excursion (numerator) when the vessel is compressed. Given that the excursion (numerator) was comparatively stable, this suggests little change in the underlying elastic modulus of the vessel wall with this mild degree of surface pressure. If this is the case, the excursion may be a more reliable measure, and the excursion divided by the pulse pressure may provide a parameter that can be used as a surrogate for vessel wall elastic modulus.<sup>51</sup>

Our initial motivation for performing this study came from recognizing that human factors may influence measurement during development of this software. While the study is relatively small in number (10 datasets using 10 trained users), the lessons learned have been important. It is clear from this detailed study on user-induced variation and potential solutions which may address variation that there is a need to define rules and algorithms to increase uniformity in point selection and hence increase accuracy and reproducibility of the automated measurement of vessel distensibility. Our first steps in semiautomated measurement were able to do this. Our results are also influencing plans for future clinical studies, reinforcing the need to study the impact of these measurement algorithms. We now have ongoing studies aimed to further develop and test these automated methods to support larger clinical studies. A recognized limitation is that all our subjects had ESRD, and we plan future studies with controls and other disease groups to further evaluate these distensibility measurements.

## Conclusions

We present our continuing effort to develop and optimize noninvasive, reproducible, and accurate technology to help predict factors influencing the creation and maturation of a functional mature AVF. The overarching goal is to enhance vascular access and hemodialysis maintenance/care for CKD and ESRD patients. This study identifies user-based point selection as a significant source of variation. There is also an observable BTB physiologic variation in the circumferential vessel wall strain (distensibility). We have developed semiautomated methods to reduce user-induced variation that preserve

physiologic measurement variation. These methods also increase the ease of use by simplifying user input. Additional work has resulted in a user interface that will also simplify use. The 2 methods show differences in their correlation level and bias when compared with reference (median) measurements. Studies are in progress to understand the impact of differences between methods. Our research plans include data and software sharing agreements with additional investigators in other institutions to expand clinical testing and further develop the methods. We also plan to expand testing the applications in peripheral vascular disease (carotid and lower extremities). Further investigation will determine where vascular strain measurements may be helpful in the diagnosis of stenotic (diseased) and nonstenotic (healthy) vessels, along with studies to evaluate the potential role of vascular strain in predicting and improving clinical outcomes.

## References

1. Allon M. Current management of vascular access. *Clin J Am Soc Nephrol* 2007; 2:786–800.
2. Ravani P, Palmer SC, Oliver MJ, et al. Associations between hemodialysis access type and clinical outcomes: a systematic review. *JASN*. 2013; 24:465–473.
3. Allon M, Ornt DB, Schwab SJ, et al. Factors associated with the prevalence of arteriovenous fistulas in hemodialysis patients in the HEMO study. Hemodialysis (HEMO) study group. *Kidney Int* 2000; 58:2178–2185.
4. Siddiqui MA, Ashraff S, Carline T. Maturation of arteriovenous fistula: analysis of key factors. *Kidney Res Clin Pract* 2017; 36: 318–328.
5. Roy-Chaudhury P, Kelly BS, Zhang J, et al. Hemodialysis vascular access dysfunction: from pathophysiology to novel therapies. *Blood Purif* 2003; 21:99–110.
6. Online United States Renal Data System. 2018 USRDS annual Data Report: Epidemiology of Kidney Disease in the United States. National Institutes of Health, National Institute of Diabetes and Digestive and Kidney Diseases, Bethesda, MD. 2018. <https://www.usrds.org/annual-data-report/previous-adrs/>. Accessed October 7, 2021.
7. Huber TS, Ozaki CK, Flynn TC, et al. Prospective validation of an algorithm to maximize native arteriovenous fistulae for chronic hemodialysis access. *J Vasc Surg* 2002; 36:452–459.
8. Jemcov TK. Morphologic and functional vessels characteristics assessed by ultrasonography for prediction of radiocephalic fistula maturation. *J Vasc Access* 2013; 14:356–363.

9. Ladenheim ED, Lulic D, Lum C, et al. First-week postoperative flow measurements are highly predictive of primary patency of radio-cephalic arteriovenous fistulas. *J Vasc Access* 2016; 17:307–312.
10. Siddiqui MA, Ashraff S, Santos D, et al. Predictive parameters of arteriovenous fistula maturation in patients with end-stage renal disease. *Kidney Res Clin Pract* 2018; 37:277–286.
11. Biswas R, Patel P, Park DW, et al. Venous Elastography: validation of a novel high-resolution ultrasound method for measuring vein compliance using finite element analysis. *Seminars in Dialysis*. 2010; 23:105–109.
12. Robbin ML, Greene T, Cheung AK, et al. Hemodialysis fistula maturation study group. Arteriovenous fistula development in the first 6 weeks after creation. *Radiology* 2016; 279:620–629.
13. Robbin ML, Greene T, Allon M, et al. Hemodialysis fistula maturation study group. Prediction of arteriovenous fistula clinical maturation from postoperative ultrasound measurements: findings from the hemodialysis fistula maturation study. *J Am Soc Nephrol* 2018; 29:2735–2744.
14. Belmont B, Park DW, Weitzel WF, et al. An open-source ultrasound software for diagnosis of fistula maturation. *ASAIO J* 2018; 64:70–76.
15. Belmont B, Park DW, Shih A, et al. A pilot study to measure vascular compliance changes during fistula maturation using open-source software. *J Vasc Access* 2019; 20:41–45.
16. Weitzel WF, Rajaram N, Zheng Y, et al. Ultrasound speckle tracking to detect vascular distensibility changes from angioplasty and branch ligation in a radio-cephalic fistula: use of novel open source software [published online ahead of print, 2020 Sep 26]. *J Vasc Access* 2020. <https://doi.org/10.1177/1129729820959910>.
17. Weitzel WF, Thelen BJ, Rajaram N, et al. Detecting high-resolution intramural vascular wall strain signals using DICOM data [published online ahead of print may 28, 2021]. *ASAIO J*. <https://doi.org/10.1097/MAT.0000000000001490>.
18. Funes-Lora MA, Thelen BJ, Shih AJ, et al. Ultrasound measurement of vascular Distensibility based on edge detection and speckle tracking using ultrasound DICOM data. *ASAIO J*. 2022; 68:112–121. <https://doi.org/10.1097/MAT.0000000000001548>.
19. Barr RG, Nakashima K, Amy D, et al. WFUMB guidelines and recommendations for clinical use of ultrasound elastography: part 2: breast. *Ultrasound Med Biol* 2015; 41:1148–1160.
20. Barr RG, Cosgrove D, Brock M, et al. WFUMB guidelines and recommendations on the clinical use of ultrasound elastography: part 5. Prostate. *Ultrasound Med Biol* 2017; 43:27–48.
21. Cosgrove D, Barr R, Bojunga J, et al. WFUMB guidelines and recommendations on the clinical use of ultrasound elastography: part 4. Thyroid. *Ultrasound Med Biol* 2017; 43:4–26.
22. Ferraioli G, Filice C, Castera L, et al. WFUMB guidelines and recommendations for clinical use of ultrasound elastography: part 3: liver. *Ultrasound Med Biol* 2015; 41:1161–1179.
23. Belmont B, Kessler R, Theyyanni N, et al. Continuous inferior vena cava diameter tracking through an iterative Kanade-Lucas-Tomasi-based algorithm. *Ultrasound Med Biol* 2018; 44:2793–2801.
24. Park DW, Richards MS, Rubin JM, Hamilton J, Kruger GH, Weitzel WF. Arterial elasticity imaging: comparison of finite-element analysis models with high-resolution ultrasound speckle tracking. *Cardiovasc Ultrasound* 2010; 8:22. <https://doi.org/10.1186/1476-7120-8-22>.
25. Park DW, Kruger GH, Rubin JM, et al. In vivo vascular wall shear rate and circumferential strain of renal disease patients. *Ultrasound Med Biol* 2013; 39:241–252.
26. Thijssen DHJ, Bruno RM, van Mil ACCM, et al. Expert consensus and evidence-based recommendations for the assessment of flow-mediated dilation in humans. *Eur Heart J* 2019; 40:2534–2547.
27. Weitzel WF, Kim K, Rubin JM, et al. Renal advances in ultrasound elasticity imaging: measuring the compliance of arteries and kidneys in end-stage renal disease. *Blood Purif* 2005; 23:10–17.
28. Weitzel WF, Kim K, Henke PK, et al. High-resolution ultrasound speckle tracking may detect vascular mechanical wall changes in peripheral artery bypass vein grafts. *Ann Vasc Surg* 2009; 23:201–206.
29. Weitzel WF, Rajaram N, Zheng Y, et al. Ultrasound speckle tracking to detect vascular distensibility changes from angioplasty and branch ligation in a radio-cephalic fistula: use of novel open-source software [published online ahead of print sept 26, 2020]. *J Vasc Access*. <https://doi.org/10.1177/1129729820959910>.
30. Ittermann T, Richter A, Junge M, et al. Variability of thyroid measurements from ultrasound and Laboratory in a Repeated Measurements Study. *Eur Thyroid J* 2020; 10:140–149.
31. Kishimoto R, Kikuchi K, Koyama A, et al. Intra- and inter-operator reproducibility of US point shear-wave elastography in various organs: evaluation in phantoms and healthy volunteers. *Eur Radiol* 2019; 29:5999–6008.
32. Sarris I, Ioannou C, Chamberlain P, et al. International fetal and newborn growth consortium for the 21st century (INTERGROWTH-21st). Intra- and interobserver variability in fetal ultrasound measurements. *Ultrasound Obstet Gynecol* 2012; 39:266–273.
33. Welliver C, Cardona-Grau D, Elebyjian L, et al. Surprising inter-observer and intra-observer variability in pediatric testicular ultrasound volumes. *J Pediatr Urol* 2019; 15:386.e1–386.e6.
34. Fraquelli M, Rigamonti C, Casazza G, et al. Reproducibility of transient elastography in the evaluation of liver fibrosis in patients with chronic liver disease. *Gut* 2007; 56:968–973. <https://doi.org/10.1136/gut.2006.111302>.
35. Liu Z, Bai Z, Huang Z, et al. Interoperator reproducibility of carotid elastography for identification of vulnerable atherosclerotic plaques. *IEEE Trans Ultrason Ferroelectr Freq Control* 2019; 66:505–516. <https://doi.org/10.1109/TUFFC.2018.2888479>.
36. Cosgrove DO, Berg WA, Doré CJ, et al. Shear wave elastography for breast masses is highly reproducible. *Eur Radiol* 2012; 22:1023–1032. <https://doi.org/10.1007/s00330-011-2340-y>.

37. Yoon JH, Kim MH, Kim EK, Moon HJ, Kwak JY, Kim MJ. Interobserver variability of ultrasound elastography: how it affects the diagnosis of breast lesions. *AJR Am J Roentgenol* 2011; 196:730–736. <https://doi.org/10.2214/AJR.10.4654>.
38. Lim DJ, Luo S, Kim MH, Ko SH, Kim Y. Interobserver agreement and intraobserver reproducibility in thyroid ultrasound elastography. *AJR Am J Roentgenol* 2012; 198:896–901. <https://doi.org/10.2214/AJR.11.7009>.
39. Milner J, Arezina J. The accuracy of ultrasound estimation of fetal weight in comparison to birth weight: a systematic review. *Ultrasound* 2018; 26:32–41.
40. Hoefler IE, den Adel B, Daemen MJ. Biomechanical factors as triggers of vascular growth. *Cardiovasc Res* 2013; 99:276–283.
41. Marques O. *Practical Image and Video Processing Using MATLAB*. 1st ed. Hoboken, NJ: John Wiley & Sons, Inc.; 2011.
42. McAndrew A. *A Computational Introduction to Digital Image Processing*. 2nd ed. Boca Raton, FL: Chapman and Hall/CRC; 2016.
43. Antón-Canalis L, Hernández-Tejera M, Sánchez-Nielsen E. AddCanny: edge detector for video processing. In: Blanc-Talon J, Philips W, Popescu D, Scheunders P (eds). *Advanced Concepts for Intelligent Vision Systems. ACIVS 2006. Lecture Notes in Computer Science*. Vol 4179. Berlin, Heidelberg: Springer; 2006. [https://doi.org/10.1007/11864349\\_46](https://doi.org/10.1007/11864349_46).
44. Majumder A, Gopi M. *Introduction to Visual Computing: Core Concepts in Computer Vision, Graphics, and Image Processing*. 1st ed. Boca Raton, FL: Chapman and Hall/CRC; 2018.
45. Middleton L, Sivaswamy J. *Hexagonal Image Processing: A Practical Approach. Advances in Computer Vision and Pattern Recognition*. 1st ed. London: Springer-Verlag; 2005.
46. Sobel, I and Feldman G. An isotropic 3X# image gradient operator [presentation]. The Stanford Artificial Intelligence Laboratory; 1968.
47. Farneback, G. Two-frame motion estimation based on polynomial expansion. Paper presented at Proceedings of the Scandinavian Conference on Image Analysis; 2003; pp. 363–370. [https://doi.org/10.1007/3-540-45103-X\\_50](https://doi.org/10.1007/3-540-45103-X_50)
48. Van Rossum, G, Drake, FL. *Python 3 Reference Manual*. Scotts Valley, CA: CreateSpace; 2009. <https://www.python.org/>
49. Stergiou GS, Kyriakoulis KG, Stambolliu E, et al. Blood pressure measurement in atrial fibrillation: review and meta-analysis of evidence on accuracy and clinical relevance. *J Hypertens* 2019; 37:2430–2441.
50. Xie L, Di X, Zhao F, et al. Increased respiratory modulation of blood pressure in hypertensive patients. *Front Physiol* 2019; 10: 1111. <https://doi.org/10.3389/fphys.2019.01111>.
51. Reusser M, Hunter KS, Lammer SR, et al. Validation of a pressure diameter method for determining modulus and strain of collagen engagement for long branches of bovine pulmonary arteries. *J Biomech Eng* 2012; 134:545011–545017.